Reanalysis of bubble chamber measurements of muon-neutrino induced single pion production

Callum Wilkinson, Philip Rodrigues, Susan Cartwright, Lee Thompson, and Kevin McFarland

Phys. Rev. D **90**, 112017 — Published 24 December 2014

DOI: 10.1103/PhysRevD.90.112017

Reanalysis of bubble chamber measurements of muon-neutrino induced single pion production

Callum Wilkinson,[1] Philip Rodrigues,[2] Susan Cartwright,[1] Lee Thompson,[1] and Kevin McFarland[2]

[1] *University of Sheffield*
[2] *University of Rochester*

(Dated: December 8, 2014)

There exists a longstanding disagreement between bubble chamber measurements of the single pion production channel $\nu_\mu p \to \mu^- p\pi^+$ from the Argonne and Brookhaven National Laboratories. We digitize and reanalyse data from both experiments to produce cross-section ratios for various interaction channels, for which the flux uncertainties cancel, and find good agreement between the experiments. By multiplying the cross-section ratio by the well-understood charged current quasi-elastic cross-section on free nucleons, we extract single-pion production cross-sections which do not depend on the flux normalization predictions. The $\nu_\mu p \to \mu^- p\pi^+$ cross-sections we extract show good agreement between the ANL and BNL datasets.

I. INTRODUCTION

Single pion production by neutrinos is an important process at neutrino energies around 1 GeV, where the dominant production mechanism is via the production and subsequent decay of hadronic resonances. In neutrino oscillation experiments, neutral-current neutral pion production is a background to ν_e charged-current events in $\nu_\mu \to \nu_e$ measurements, while charged-current events producing charged pions contribute to ν_μ disappearance measurements, either as background in analyses which select quasi-elastic events, or as signal in analyses which use an inclusive charged-current selection.

Predictions of single pion production on the nuclei used in neutrino oscillation experiments usually factorize the modelling into three parts: the neutrino-nucleon cross section; additional effects due to the nucleon being bound in the nucleus; and the "final state interactions" (FSI) of hadrons exiting the nucleus. Experimental knowledge of the neutrino-nucleon cross section for single pion production, in the 100 MeV to few-GeV neutrino energy range relevant for current and planned oscillation experiments, is sparse, coming from bubble chamber experiments with hydrogen or deuterium targets with low statistics. In particular, data from the 12 ft bubble chamber at Argonne National Laboratory (ANL) and the 7 ft bubble chamber at Brookhaven National Laboratory (BNL) for the leading single pion production process $\nu_\mu p \to \mu^- p\pi^+$ differ in normalization by 30–40 %. This data is used to constrain the axial form factor for pion production on free nucleons, which cannot be constrained by electron scattering data, so this discrepancy leads to large uncertainties in the predictions for oscillation experiments [1–6], as well as in interpretation of data taken on nuclear targets [7].

Resolving this discrepancy will be vital for current and future neutrino oscillation experiments, which have very stringent systematic error requirements [8, 9], but current neutrino cross section measurements are taken on nuclear targets such as carbon and oxygen, where it is difficult to disentangle the neutrino-nucleus cross section from the effects of the nucleus and FSI. In this context, it is worthwhile to revisit the ANL and BNL datasets to look for possible consistency. Graczyk *et al.* have found consistency in the datasets by carefully considering normalization uncertainties [1][10] and deuteron nuclear effects. In this paper, we present a complementary approach in which we consider ratios of event rates for different processes in the ANL and BNL experiments, in which normalization uncertainties cancel. By multiplying the event rate ratio by an independent measurement of the cross section of the denominator, we obtain a measurement of the single-pion production cross section. In essence, this method amounts to using the denominator cross section as the factor which converts an event rate into a cross section, where the original analyses used a prediction of the neutrino flux for the same purpose.

The paper is organized as follows. In Section II, we describe the method for obtaining the data from the original papers. A discussion of the sources of error for these datasets is in Section III. In Section IV, we present the ratios of event rates for various processes. Then these are used in Section V to extract CC-inclusive and $\nu_\mu p \to \mu^- p\pi^+$ cross-sections, where we find good agreement between ANL and BNL. Our conclusions are presented in Section VI.

II. OBTAINING DATA

A literature review of the ANL and BNL cross-section papers produces a wealth of data. For this analysis, corrected event rates as a function of the neutrino energy, E_ν, are required. Corrected event rates are obtained from the raw (measured) event rates by estimating detector inefficiencies, and subtracting background processes. As we are interested in $\nu_\mu - \mathrm{D}_2$ interactions, we remove data from hydrogen fills of the experiments. This section discusses how the datasets used in this analysis were obtained. All data published as histograms have been digitized using the engauge digitizer tool [11]. The discrepancy between the published event rates and the event rate obtained by integrating the digitized histograms is

less than 1%. The effect of ditigization on the shape of the distributions is assumed to be small.

A. ANL 12 ft bubble chamber

A description of the experimental setup for the 12 ft bubble chamber at Argonne National Laboratory (ANL) can be found in [12]. Additional details of the event reconstruction and classification algorithms used can be found in [13] and [14]. In the ANL experiment, data was initially taken with a hydrogen fill of the bubble chamber, then data was taken with a deuterium fill for the remainder of the experiment [12]. Event rates are only available as a combination of both hydrogen and deuterium fills of the detector, so care must be taken to remove the hydrogen component. Published cross-sections are given using two different datasets, which we refer to here as the ANL partial and full datasets. The partial dataset is described in Reference [12], and is approximately 30% of the final dataset. The full dataset is described in Reference [13]. Events on hydrogen comprise approximately 2% (6%) of the total for the full (partial) dataset.

The raw event rate for the $\nu_\mu p \to \mu^- p\pi^+$ channel is given in [13] using the complete ANL dataset. No invariant mass cuts were used when selecting these events. The published (digitized) number of events before corrections is 871 (843.2); we scale the digitized distribution to the published corrected event rate of 1115.0. A small subset of the data comes from the earlier hydrogen fill of the detector, which contributes 90 $\nu_\mu p \to \mu^- p\pi^+$ events (corrected) [14].

The corrected event rates for the CCQE and CC-inclusive channels with the partial ANL datset are taken from [14]. The events are presented as four samples, as summarized in Table I: in later stages of the analysis, the digitized distributions are scaled to match the published event rate. The CC-inclusive contribution from proton interactions is also scaled to remove the 102 interactions on hydrogen (of 457 total).

Dataset	Channel	Digitized	Published
Partial	$\nu n \to \mu^- p$	834.6	833
	$\nu p \to \mu^- p\pi^+$	395.9	398
	$\nu n \to \mu^- X^+$	1139.2	1150
	$\nu p \to \mu^- X^{++}$	453.2	457
Full	$\nu p \to \mu^- p\pi^+$	843.2	871

TABLE I: Numbers of events for each of the ANL samples as published by ANL and as digitized for this work.

As the $\nu_\mu p \to \mu^- p\pi^+$ event rate is given for both the partial and final ANL datasets, the ratio can be used to scale the CCQE and CC-inclusive samples from the partial dataset to the statistics of the full ANL dataset. The digitized ANL data for all channels considered, with all corrections applied, are given in Figure 1a, where the errors are statistical only.

B. BNL 7 ft bubble chamber

A description of the experimental setup of the 7 ft bubble chamber at Brookhaven National Laboratory (BNL), and a description of the event reconstruction and classification algorithms, can be found in References [15–18]. Although events were initially taken with a hydrogen fill of the bubble chamber, most BNL results are separated into hydrogen and deuterium measurements. As for ANL, published BNL cross-sections are given using two different datasets, which we refer to here as the BNL partial and full datasets. The partial dataset is described in Reference [15], and is approximately 30% of the final dataset. The full dataset is described in Reference [18].

The published (digitized) number of uncorrected CCQE events on deuterium, using the full BNL dataset, is 2684 (2693.3) [17]; we scale the digitized distribution by the published correction factor of 1.11 to obtain the corrected event rate.

For $\nu_\mu p \to \mu^- p\pi^+$ with no cut on the invariant mass, the published (digitized[1]) number of raw events, for the complete BNL dataset, is 1610 (1534.7) [18] and the digitized distribution is scaled by the published correction factor of 1.123 to obtain the corrected event rate. The $\nu_\mu p \to \mu^- p\pi^+$ results are also presented in Reference [17] as well as a $\nu_\mu p \to \mu^- p\pi^+$ /CCQE ratio, but these results have a hadronic invariant mass cut, $W < 1.4\,\text{GeV}$, so have not been used for this analysis.

The uncorrected CC-inclusive event rate for $E_\nu \leq 14\,\text{GeV}$ using approximately 30% of the total deuterium data is 3723 published [16] and 3685.3 digitized. The correction factor for BNL CC-inclusive events is not explicitly given, but we can identify three corrections that should be applied to CC-inclusive data:

- Scanning-measuring efficiency, $f_1 = 1.11 \pm 0.02$ [18],
- NC Background, $f_2 = 0.94 \pm 0.01$ [15],
- H_2 contamination in D_2, $f_3 = 0.96$.[2]

These corrections are combined to give a total correction factor $f \equiv f_1 \times f_2 \times f_3 = 1.00$ for the CC-inclusive dataset.

---

[1] The data was only extracted for $0 \leq E_\nu \leq 6$ GeV, as it was difficult to distinguish higher energy bins reliably due to the quality of the published histogram, and so does not contain all of the events in the quoted raw event number. For this reason, the digitized histogram was not scaled to match the quoted event rate.

[2] The correction factor for H_2 contamination in D_2 is given as 0.87 ± 0.02 in [18], for interactions off a proton. In [16], BNL measure the ratio of CC-inclusive reactions off a neutron to those off a proton as $\sigma(\nu n)/\sigma(\nu p) = 1.95 \pm 0.10$. We combine these to arrive at an estimate of the correction factor for H_2 contamination in D_2 for CC-inclusive events, $f_3 = 0.96$.

Dataset	Channel	Digitized	Published
Partial	$\nu n \to \mu^- p$	—	1276
	$\nu N \to \mu^- X$	3685.3	3723
Full	$\nu n \to \mu^- p$	2693.3	2684
	$\nu p \to \mu^- p \pi^+$	1534.7	1610

TABLE II: Numbers of events for each of the BNL samples as published by BNL and as digitized for this work. Note that it was not necessary to digitize the CCQE event rate for the partial BNL dataset.

The raw event rates are summarized in Table II for all processes. As the number of CCQE events is given for both the partial and complete datasets, the ratio of the two can be used to scale the CC-inclusive event rate up to the statistics of the full BNL deuterium dataset. The digitized BNL data for all channels, with all corrections applied, are given in Figure 1b, shown with statistical errors only.

III. ERROR ANALYSIS

Throughout this work, only statistical errors are considered, which are the dominant source of error for these low-statistics bubble chamber datasets. Flux normalization errors are the second largest errors in the original ANL and BNL analyses, at around 15-20%. These are not considered here because they cancel by construction in ratios of event rates.

There are additional errors on the overall normalization of all channels, which are introduced by the background subtraction and correction for detector effects; these are summarized for BNL in [17], and can be inferred for ANL from [14]. A conservative estimate of the normalisation error for both experiments would be approximately 5 %. It is also likely that many of the sources of uncertainty are common between interaction channels, and would cancel in the ratios calculated here, but a full error analysis is not possible.

There is also an error on the reconstructed neutrino energy, which is estimated for BNL to be $\frac{\Delta E_\nu}{E_\nu} \sim 2\,\%$ for CCQE and $\nu_\mu p \to \mu^- p \pi^+$ events [15], and $\sim 5\,\%$ for other charged current production channels which are not kinematically overconstrained. ANL also quote an error of $\frac{\Delta E_\nu}{E_\nu} \leq 5\,\%$ for the harder to reconstruct channels, but do not quote an error on kinematically overconstrained channels [13]. As the uncertainty on E_ν largely comes from uncertainty in the beam direction, and BNL (ANL) quote small uncertainties $\pm 0.5°$ [15] ($\pm 1.0°$ [14]), we conclude that this error will be small, and $\frac{\Delta E_\nu}{E_\nu} \leq 5\,\%$ for all channels considered here.

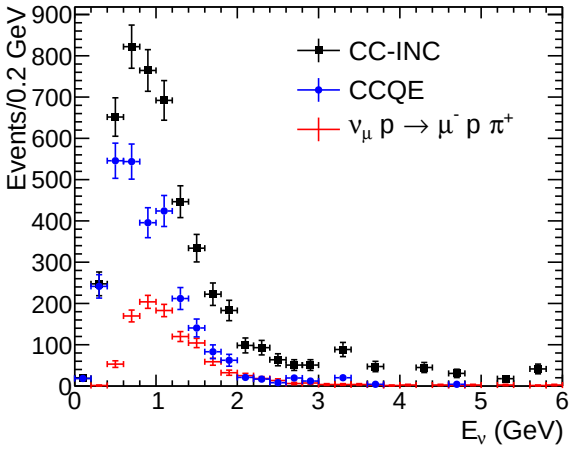

(a) ANL

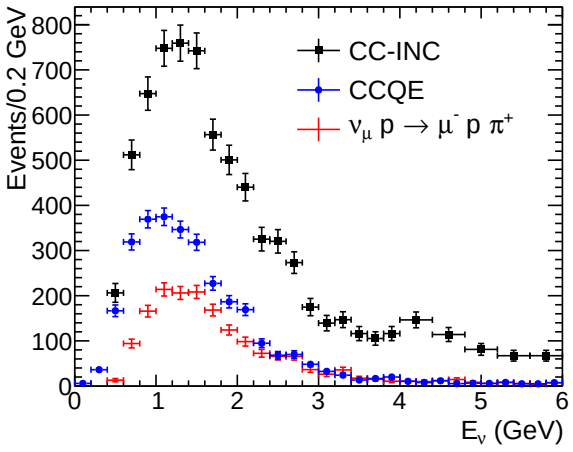

(b) BNL

FIG. 1: The digitized event rates on deuterium for the three interaction channels CCQE, $\nu_\mu p \to \mu^- p \pi^+$ and CC-inclusive, as a function of the reconstructed neutrino energy E_ν. The errors are statistical only. Both ANL and BNL event rates and errors have been scaled when necessary to the statistics of their full deuterium samples.

IV. E_ν-DEPENDENT EVENT RATE RATIOS

The number of events $N_X(E)$ for a given process X in an energy bin E is the product of flux $\Phi(E)$ and cross section $\sigma_X(E)$, so the ratio of corrected event rates for different channels is equal to the ratio of the cross-section for those channels. More importantly, in this ratio the flux and associated flux uncertainties cancel. So by taking the ratios between channels, it is possible to look for consistency in the ANL and BNL results regardless of possible problems with their flux predictions.

There is very good agreement between ANL and BNL in the ratio $\frac{\mathrm{CC1}\pi^+}{\mathrm{CCQE}}$, as shown in Figure 2. This is con-

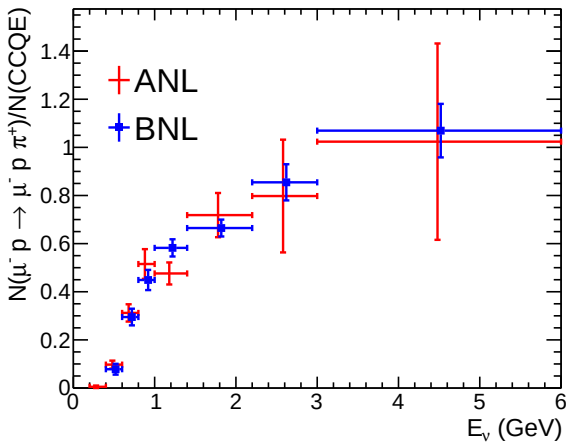

FIG. 2: Ratio of $\nu_\mu p \to \mu^- p\pi^+$ to CCQE events as a function of E_ν for both ANL and BNL.

trary to expectation, given the discrepancy in the published $\nu_\mu p \to \mu^- p\pi^+$ results, and suggests that the cause of the discrepancy is the flux prediction used to extract cross-sections from each experiment. This conclusion is supported by other analyses [1][10], which found that the ANL and BNL results are compatible within their flux normalization uncertainties.

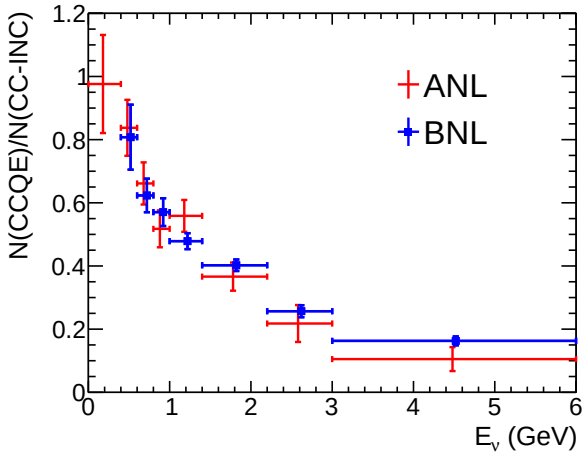

FIG. 3: Ratio of CCQE to CC-inclusive events as a function of E_ν for both ANL and BNL.

We also find reasonable agreement in the ratio $\frac{\mathrm{CCQE}}{\mathrm{CC-INC}}$ as shown in Figure 3, and in the ratio $\frac{\mathrm{CC1}\pi^+}{\mathrm{CC-INC}}$ as shown in Figure 4. However, CC-inclusive selections are more challenging than the exclusive channels CCQE and $\nu_\mu p \to \mu^- p\pi^+$. This is due to the high track multiplicity events which are included in CC-inclusive samples, and which have large uncertainties on their measuring efficiencies [18]. This can also be inferred from [14] Table 1, where the corrected event rates for high track multiplicity events have large uncertainties. We also note that the correction factor for the BNL CC-inclusive dataset is based on our own estimate given in Section II B, as it was not published.

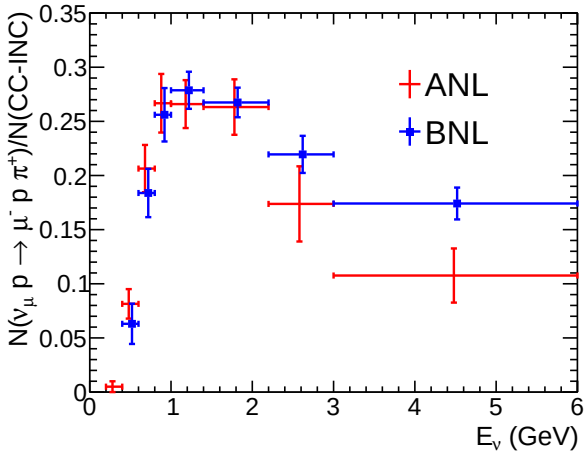

FIG. 4: Ratio of $\nu_\mu p \to \mu^- p\pi^+$ to CC-inclusive events as a function of E_ν for both ANL and BNL.

V. CONVERSION TO CROSS-SECTIONS USING KNOWN CCQE CROSS SECTION

As the CCQE cross-section on deuterium is relatively well understood, it is possible to produce $\nu_\mu p \to \mu^- p\pi^+$ and CC-inclusive cross-section predictions by multiplying the cross-section ratios presented in the previous section by the CCQE cross-section. Effectively, this removes the ANL and BNL flux uncertainties, and replaces it with the theoretical uncertainty on the CCQE cross-section prediction, which is small (and has not been included in the plots presented here). The errors on our derived cross-sections are statistical only and may be larger than for the published ANL and BNL results, as the statistical error for two channels has been combined in quadrature.

The $\nu_\mu - D_2$ CCQE cross-section prediction we use is produced using GENIE 2.8 [19], which is an implementation of the Llewellyn Smith [20] model, the expression for which is given in Equation 3.18 of reference [20]. A dipole axial form factor is assumed, with an axial mass, $M_A = 0.99\,\mathrm{GeV}$. Since this value is based mainly on fits to the shapes of Q^2 distributions [21], it is independent of the ANL and BNL flux normalization, so our only assumption is that the Llewelyn Smith model provides a reasonable description of CCQE neutrino–nucleon scattering. We note that other analyses produce consistent values of M_A [22][23]. The cross-section spline used in this analysis has been reproduced in Figure 5.

The CC1π^+ cross-sections from both ANL and BNL, produced by multiplying the $\frac{\mathrm{CC1}\pi^+}{\mathrm{CCQE}}$ ratio by the GENIE CCQE cross-section, are shown in Figure 6. The GENIE Δ^{++} cross-section has been included for com-

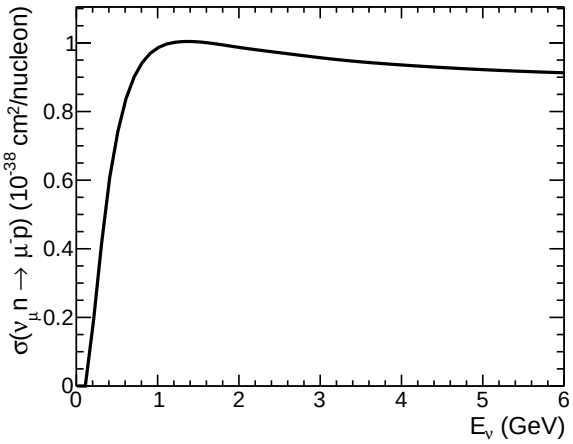

FIG. 5: The default CCQE cross-section prediction for $\nu_\mu - \mathrm{D}_2$, taken from GENIE 2.8 using the default model parameters.

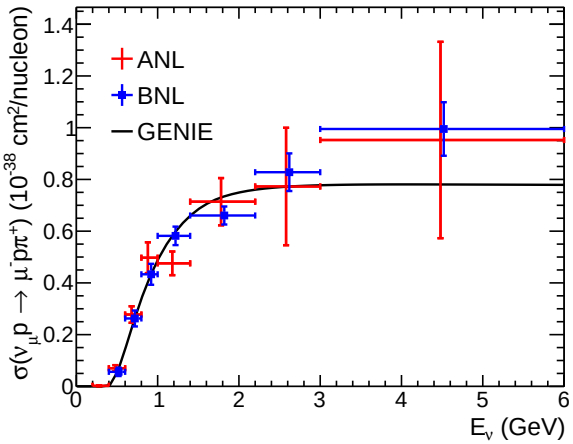

FIG. 6: Comparison of the CC1π^+ cross-sections for both ANL and BNL, obtained by multiplying the ratio $\frac{\mathrm{CC1}\pi^+}{\mathrm{CCQE}}$ by the GENIE CCQE cross-section prediction for $\nu_\mu - \mathrm{D}_2$ interactions. The GENIE Δ^{++} cross-section prediction has been added for reference, but was not used when producing the cross-section.

parison, as this resonance makes the biggest contribution. However, higher order resonances also contribute to the measurements, particularly at high neutrino energies, so the measurements are expected to deviate from the GENIE predictions at high E_ν. Note that there is no invariant mass cut on the distributions used to extract the $\nu_\mu p \to \mu^- p\pi^+$ cross-sections produced in this work. The GENIE Δ^{++} cross-section is an implementation of the Rein–Sehgal model [24], with a resonant axial mass, $M_A^{RES} = 1.12\,\mathrm{GeV}$ taken from global fits carried out in reference [22].

It is interesting to compare the extracted $\nu_\mu p \to \mu^- p\pi^+$ cross-sections with those published by ANL and

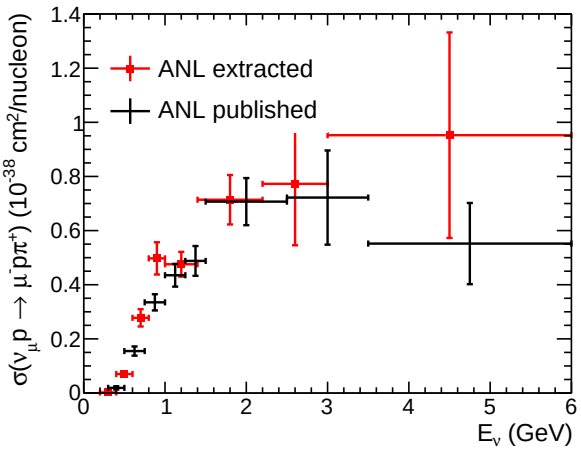

(a) ANL

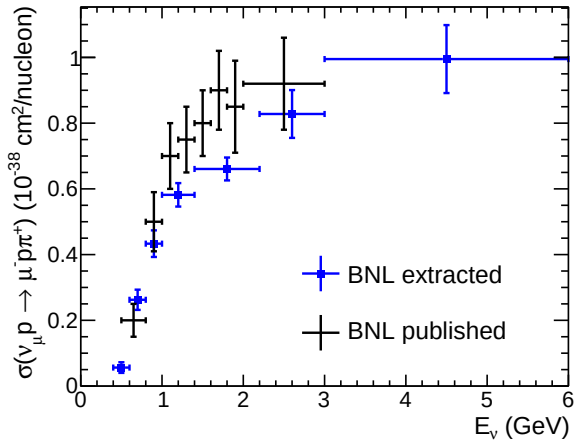

(b) BNL

FIG. 7: Comparison of the CC1π^+ cross-sections for both ANL and BNL, compared with the published CC1π^+ cross-section from each experiment. Note that the published cross-section includes the flux normalization uncertainty.

BNL, as shown in Figure 7. In the neutrino energy range where ANL and BNL disagree most strongly, $1 \leq E_\nu \leq 2$ GeV, the extracted BNL cross-section differs significantly from the published distribution (Figure 7b), whereas the extracted ANL results show reasonable agreement with the published ANL data (Figure 7a). The comparisons shown in Figure 7 agree well with the observation made in another analysis, that good agreement between the ANL and BNL single pion production data, and theoretical prediction, could be achieved by supposing that the BNL cross-sections were overestimated by 30% [25].

The published and extracted ANL and BNL $\nu_\mu p \to \mu^- p\pi^+$ cross-sections are compared with all available datasets on hydrogen and deuterium targets taken at higher neutrino energies in Figure 8. The additional datasets are from the Fermilab 15 ft bubble chamber

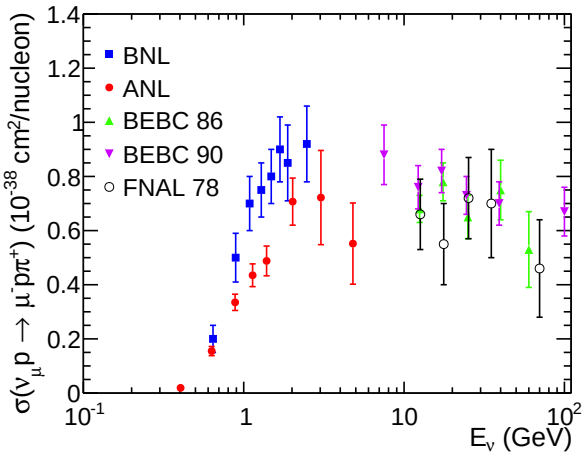

(a) Published

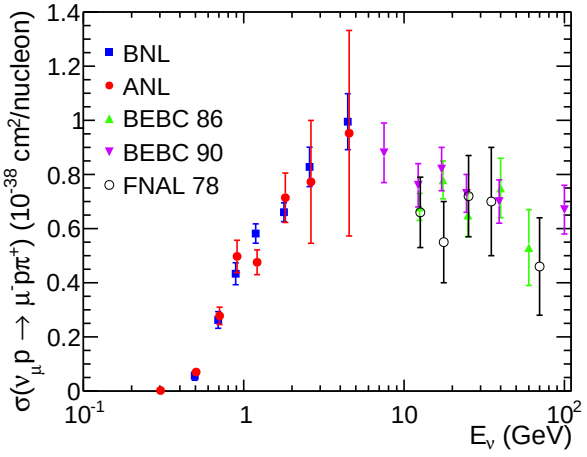

(b) This analysis

FIG. 8: The published and extracted ANL and BNL data are compared with other measurements of $\nu_\mu p \to \mu^- p\pi^+$ on hydrogen or deuterium targets [26–28]. Note that the ANL and BNL data have no invariant mass cut, whereas the other datasets have an invariant mass cut of $W \leq 2\,\text{GeV}$.

filled with hydrogen (FNAL 1978) [26], the Big European Bubble Chamber (BEBC) filled with hydrogen (BEBC 1986) [27], and with deuterium (BEBC 1990) [28]. One important caveat is that the other datasets have an invariant mass cut of $W < 2\,\text{GeV}$, whereas, in this analysis, the ANL and BNL datasets used have no invariant mass cut. It is clear that the extracted cross-sections presented here agree well with the global dataset.

For completeness, Figure 9 shows the CC-inclusive cross-sections from both ANL and BNL, produced by multiplying the $\frac{\text{CC}-\text{inclusive}}{\text{CCQE}}$ ratio by the GENIE CCQE cross-section. However, we note again that the correction factor applied to the BNL CC-inclusive dataset was estimated as it was not explicitly given in a BNL publication.

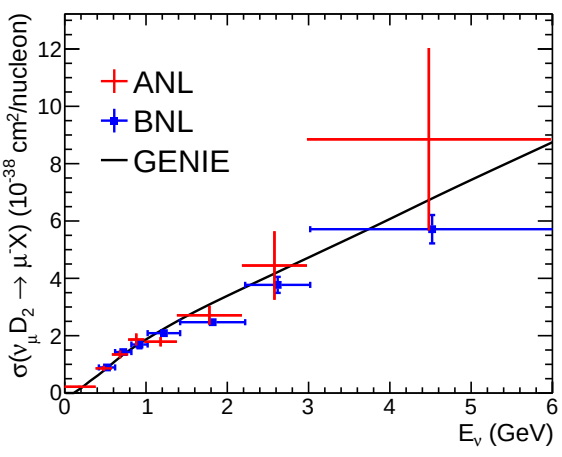

FIG. 9: Comparison of the $\nu_\mu p \to \mu^- p\pi^+$ cross-sections for both ANL and BNL, obtained by multiplying the ratio $\frac{\text{CC}-\text{inclusive}}{\text{CCQE}}$ by the GENIE CCQE cross-section prediction for $\nu_\mu - \text{D}_2$ interactions. The GENIE CC-inclusive cross-section prediction has been added for comparison, but was not used when producing the cross-sections.

VI. CONCLUSIONS

In this work we have digitized and reanalysed ANL and BNL data for $\nu_\mu - \text{D}_2$ scattering, and demonstrated that there is good agreement between ANL and BNL for the ratio $\sigma_{\nu_\mu p \to \mu^- p\pi^+}/\sigma_{\text{CCQE}}$. This indicates that the outstanding ANL–BNL single pion production "puzzle" results from discrepancies in the flux predictions, which is in accordance with previous analyses of the same data [1][10], which found that ANL and BNL agree within their published flux uncertainties. Using these ratios, we exploit the fact that the CCQE cross-section for interactions on deuterium is well understood to extract $\nu_\mu p \to \mu^- p\pi^+$ cross-sections for both ANL and BNL. Although we only show statistical errors, the flux errors cancel, and the remaining normalization errors are small, and are likely to partially cancel when taking the ratio. Additional errors in the shape of the distributions from the energy resolution are likely to be small, and are unlikely to significantly distort the cross-section. Comparing our extracted results to the published ANL and BNL cross-sections, we found better agreement with ANL than BNL. However, we stress that both experiments gave large normalization uncertainties on their fluxes, so this is not indicative of a problem with the BNL results. The extracted cross-sections presented here resolve the longstanding ANL–BNL "puzzle", and should be used in future fits where this data is used to constrain the axial form factor for pion production on nucleons. The reduced error on this parameter will be of use to future neutrino oscillation measurements, and in interpreting the increasing body of single pion production data from

nuclear targets [29–35], where nuclear effects have yet to be fully understood.

We note that data from ANL and BNL is available for the subleading pion production processes $\nu_\mu + n \to \mu^- + p + \pi^0$ and $\nu_\mu + n \to \mu^- + n + \pi^+$. There is an unmeasurable particle in the final state which would make the analysis more dependent on the models used by ANL and BNL to estimate their measuring efficiencies. Analysis of these more complicated channels has been left for future work.

ACKNOWLEDGMENTS

This work developed from studies performed by the T2K experiment's neutrino interaction working group, who we thank for their encouragement and comments, and discussions at the NuInt series of conferences. We are grateful to Anthony Mann for helpful comments on an earlier presentation of this work. This material is based upon work supported by the US Department of Energy under Grant DE-SC0008475 and by the UK STFC as a PhD studentship.

[1] K.M. Graczyk, D. Kielczewska, P. Przewlocki, and J.T. Sobczyk, Phys. Rev. **D80**, 093001 (2009), arXiv:0908.2175 [hep-ph].
[2] E. Hernandez, J. Nieves, and M. Valverde, Phys. Rev. **D76**, 033005 (2007), arXiv:hep-ph/0701149 [hep-ph].
[3] T. Leitner, O. Buss, L. Alvarez-Ruso, and U. Mosel, Phys. Rev. **C79**, 034601 (2009), arXiv:0812.0587 [nucl-th].
[4] E. Hernandez, J. Nieves, M. Valverde, and M. Vicente Vacas, Phys. Rev. **D81**, 085046 (2010), arXiv:1001.4416 [hep-ph].
[5] M. Ahn *et al.* (K2K Collaboration), Phys. Rev. Lett. **90**, 041801 (2003), arXiv:hep-ex/0212007 [hep-ex].
[6] K. Abe *et al.* (T2K Collaboration), Phys. Rev. D **88**, 032002 (Aug 2013), `http://link.aps.org/doi/10.1103/PhysRevD.88.032002`.
[7] O. Lalakulich and U. Mosel, Phys. Rev. **C87**, 014602 (2013), arXiv:1210.4717 [nucl-th].
[8] C. Adams *et al.* (LBNE Collaboration)(2013), arXiv:1307.7335 [hep-ex].
[9] K. Abe *et al.* (T2K Collaboration)(2014), arXiv:1409.7469 [hep-ex].
[10] K. M. Graczyk, J. Zmuda, and J. T. Sobczyk(2014), arXiv:1407.5445 [hep-ph].
[11] M. Mitchell, "Engauge digitizer - digitizing software," Http://digitizer.sourceforge.net/, `http://digitizer.sourceforge.net/`.
[12] S. Barish, J. Campbell, G. Charlton, Y. Cho, M. Derrick, *et al.*, Phys. Rev. **D16**, 3103 (1977).
[13] G. Radecky, V. Barnes, D. Carmony, A. Garfinkel, M. Derrick, *et al.*, Phys. Rev. **D25**, 1161 (1982).
[14] S. Barish, M. Derrick, T. Dombeck, L. Hyman, K. Jaeger, *et al.*, Phys. Rev. **D19**, 2521 (1979).
[15] N. Baker, A. Cnops, P. Connolly, S. Kahn, H. Kirk, *et al.*, Phys. Rev. **D23**, 2499 (1981).
[16] N. Baker, P. Connolly, S. Kahn, M. Murtagh, R. Palmer, *et al.*, Phys. Rev. **D25**, 617 (1982).
[17] T. Kitagaki, H. Yuta, S. Tanaka, A. Yamaguchi, K. Abe, *et al.*, Phys. Rev. **D42**, 1331 (1990).
[18] T. Kitagaki, H. Yuta, S. Tanaka, A. Yamaguchi, K. Abe, *et al.*, Phys. Rev. **D34**, 2554 (1986).
[19] C. Andreopoulos, A. Bell, D. Bhattacharya, F. Cavanna, J. Dobson, *et al.*, Nucl. Instrum. Meth. **A614**, 87 (2010), arXiv:0905.2517 [hep-ph].
[20] C. Llewellyn Smith, Phys. Rept. **3**, 261 (1972).
[21] H. S. Budd, A. Bodek, and J. Arrington(2003), arXiv:hep-ex/0308005 [hep-ex].
[22] K. S. Kuzmin, V. V. Lyubushkin, and V. A. Naumov, Acta Phys. Polon. **B37**, 2337 (2006), arXiv:hep-ph/0606184 [hep-ph].
[23] K. S. Kuzmin, V. V. Lyubushkin, and V. A. Naumov, Eur. Phys. J. **C54**, 517 (2008), arXiv:0712.4384 [hep-ph].
[24] D. Rein and L. M. Sehgal, Annals Phys. **133**, 79 (1981).
[25] O. Lalakulich, T. Leitner, O. Buss, and U. Mosel, Phys. Rev. **D82**, 093001 (2010), arXiv:1007.0925 [hep-ph].
[26] J. Bell, C. Coffin, R. Diamond, H. French, W. Louis, *et al.*, Phys. Rev. Lett. **41**, 1008 (1978).
[27] P. Allen *et al.* (Aachen-Birmingham-Bonn-CERN-London-Munich-Oxford Collaboration), Nucl. Phys. **B264**, 221 (1986).
[28] D. Allasia, C. Angelini, G. van Apeldoorn, A. Baldini, S. Barlag, *et al.*, Nucl. Phys. **B343**, 285 (1990).
[29] C. Mariani *et al.* (The K2K Collaboration), Phys. Rev. D **83**, 054023 (Mar 2011), `http://link.aps.org/doi/10.1103/PhysRevD.83.054023`.
[30] S. Nakayama *et al.* (The K2K Collaboration), Physics Letters B **619**, 255 (2005), ISSN 0370-2693, `http://www.sciencedirect.com/science/article/pii/S0370269305007161`.
[31] Y. Kurimoto *et al.* (SciBooNE Collaboration), Phys. Rev. **D81**, 033004 (2010), arXiv:0910.5768 [hep-ex].
[32] A. Aguilar-Arevalo *et al.* (MiniBooNE Collaboration), Phys. Rev. **D83**, 052007 (2011), arXiv:1011.3572 [hep-ex].
[33] A. Aguilar-Arevalo *et al.* (MiniBooNE Collaboration), Phys. Rev. **D83**, 052009 (2011), arXiv:1010.3264 [hep-ex].
[34] A. Aguilar-Arevalo *et al.* (MiniBooNE Collaboration), Phys. Rev. **D81**, 013005 (2010), arXiv:0911.2063 [hep-ex].
[35] B. Eberly *et al.* (MINERvA Collaboration)(2014), arXiv:1406.6415 [hep-ex].